Hindawi

Research Article

Calculation and Analysis of Nonlinear Algorithm for Stability of Nanosilica Powder Soft Soil Pile Foundation

Jinbo Sun [ID],[1] **Li Guo** [ID],[1] **Liang Gong** [ID],[1] **Fei Zheng** [ID],[2] **and Hao Hao** [ID][3]

[1]*School of Civil Engineering, Southeast University, Jiangsu, Nanjing 211189, China*
[2]*China Construction Power and Environment Engineering Co.Ltd, Jiangsu, Nanjing 210009, China*
[3]*Management Committee of China (Nanjing) Software Valley, Jiangsu, Nanjing 210012, China*

Correspondence should be addressed to Li Guo; 201823252501041@zcmu.edu.cn

In order to reasonably evaluate the stability of the embankment supported by the rigid pile composite foundation, a nonlinear algorithm calculation and analysis method for the stability of the nanosilica powder soft soil pile foundation is proposed. First, the soft soil foundation reinforced by the composite structure of "piles (prestressed pipe piles, (cement fly-ash gravel, CFG) piles)—pile caps—geotextile pads" is analyzed through the soft soil embankment test section of the Wenfu high-speed railway. Second, the compressive modulus under one-dimensional confining compression is calculated using the layered summation method. Finally, the deep lateral deformation of the pile foundation soil is measured by an inclinometer to evaluate the actual displacement of the pile foundation soil. In the standard method, the empirical coefficient 1.1–1.7 is multiplied on the basis of the calculation result of this method to correct the calculation error. Combined with the test results, it is shown that nanosilica powder can give full play to its excellent characteristics: promoting hydration speed and hydration degree through the reaction of pozzolan refining and consuming $Ca(OH)_2$ crystals produced by cement hydration. Soft soils and modified soft soils: a certain amount of nanosilica powder can significantly improve the strength of soft soil at different ages.

1. Introduction

Due to the high strength of nanosilica powder soft soil foundation, the nonlinear lateral deformation is obvious. Although the current calculation methods are developed and there are various numerical methods, the most famous one is the finite element method, and the finite element method is also used to study the influence of lateral deformation; the most commonly used method in engineering design is still the standard layered sum method [1]. The method uses a one-dimensional compression test; under the stress state of compression modulus, the layered summation method is used to calculate the compression of soil lateral deformation; the calculation cannot consider lateral deformation caused by lateral deformation, so be on the basis of calculation results are superior to the empirical coefficient of 1.1–1.7 to correct the error of calculation and actual deformation. In addition, the lateral deformation of the foundation soil

comprehensive method is to use nonlinear or elastoplastic constitutive relation and use the finite element method to solve the consolidation theory, but this method is generally more complex and the constitutive model of the complex, model parameter test difficulty is high, the error is big, and the calculation results are not ideal, not to improve calculation accuracy. In practical engineering, it still mainly depends on the standard method of the layered summation method and empirical coefficient, which can be easily obtained by parameters [2]. However, the empirical coefficient interval of the normative method is large, and there is a lack of the scientific quantitative value method. The value is mainly subjective, and the results will vary from person to person. The accuracy needs to be improved, and its advantage is simplicity.

E-P curve is the main and easy-to-obtain test curve in soft soil engineering. On the basis of the E-P curve, combined with the constitutive theory of modern soil, it is of

great significance to establish a practical calculation method that can calculate the nonlinear lateral deformation. In the process of application, it is observed that the tangent modulus ET of soft soil changes too fast, which easily leads to the instability of calculation results. Because there is a square relation between the tangent modulus method 2Tf (1) Ierse, (1), the strength of soft soil is low, and the general stress level is high, which can easily reach or exceed 0.5 or even easily reach 0.8–0.9, so that the tangent modulus Et decreases rapidly, and the calculation results are easy to be unstable. In order to improve the stability of the calculation, the secant modulus method is proposed to calculate the lateral deformation of shear deformation, so as to increase the stability of the calculation results [3]. At the same time, in the above calculation, a complete E-P curve is needed to obtain the compression modulus ESI under different stress levels. However, the investigation and test reports of many engineering projects in actual engineering do not provide a complete E-P curve, but only provide the initial porosity ratio E0 and compression modulus ES1-2 of soft soil. Since the above two parameters are commonly used in engineering, they are relatively stable and can better reflect the characteristics of soft soil. In general soft soil, the initial porosity ratio of silty soil is $E0 = 1.0–1.5$ and that of silty soil is 1.5–2.5, and the compression modulus of soft soil is ES1-2=2.0-3.0 MPa [4]. These indexes are stable. If a practical nonlinear lateral deformation calculation method can be established from these simple physical and mechanical indexes, it will be more conducive to engineering application. On the other hand, the E-lgp relation only needs one parameter, the compression index CC, to reflect the nonlinear relation of E-p, and this relationship has been recognized by peers in the world. Therefore, if the relation of compression index CC obtained from E0 and ES1-2 can be established, the E-lgp relation can be established from CC, and the E-lgp relation is linear. The linear relation of E-lgp can reflect the nonlinear relation of E-p. In this way, the compression modulus ESI under different stress levels can be obtained from E-lgp and used to calculate the consolidated lateral deformation and shear lateral deformation, respectively, by the above method, so as to calculate the nonlinear lateral deformation of soft soil foundation. In this calculation, only the initial porosity ratio E0 and the compression modulus ES1-2 are required to reflect the deformation. This will bring great convenience to the calculation.

Soft soil is silty clay. The strength of cement soil can be increased by 5%–290% by adding nanosilica powder. As for the modification effect of other soil properties, it is necessary to discuss the strength growth mechanism of nanosilica powder. From the above analysis of the curing mechanism, it can be observed that the strengthening mechanism of nanosilica powder on soil cement mainly lies in the activity of nanosilica powder. In this regard, domestic and foreign researches continue, such as by Ding et al. The binding mechanism of heavy metals in soil treated with nanosilica powder was studied [5]. Afzali-Naniz and Mazloom studied the topology, crystal chemistry, and surface properties of nanosilica powder and nanoetched plagioclase [6]. Abd Elrahman et al. studied the effects of nanosilica powder on

soil collapse treatment in the Siwan area of Fars Province, Iran [7]. Because of the different hydration environments, the effect and the optimal dosage of nanosilicon powder will be different. For general clay and soft soil, because of the "secondary reaction" and ion exchange effect of clay particles, nanosilica powder is beneficial to improving the microstructure of cement soil, and the enhancement effect of nanosilica powder is better than that of sand and silt soil [8]. For soft soil with large organic matter content, the enhancement effect is worse. The enhancement effect of nanosilica powder on each kind of soil and the optimum dosage needs to be further studied.

2. Experimental Methods and Algorithms

2.1. Strength Test of Nanosilicate Soft Soil. The ratio scheme of the design is as follows: soft soil parameters (soft soil mass/water mass *100% is 15%); the parameters of nanosilica powder (= mass of nanosilica powder/mass of soft soil *1000%) were 0, 2.5%, 5%, 7.5%, 10%, 15%, 20%, 25%, and 30%; the ratio of nanosilica powder to soft soil (W/C = water mass/(nanosilica powder mass + soft soil mass)) was 0.45. The ages were 7, 28, and 60 days. Parallel tests were conducted for each ratio [9]. The test instrument is TSY6—IB desktop triaxial compression instrument. Test shear rate was 04 mm/min.

Figure 1 shows the relationship between the content of nanosilica powder a_w and the unconfined compressive strength q_u at various ages. As can be observed from Figure 1, the relative density parameter of silica fume is 2.2–2.5, and the strength increases linearly with the increase of nanosilicon powder content. When $a_w = 250\%$, the strength of the soil reached the maximum value of 2.81 MPa on day 7, which was 3.52 times that of the common soft soil at the same age [10]. When the age is 28 days and a_w is 30%, the maximum strength of the soil can reach 4.51 MPa, which is 3.92 times that of the common soft soil for 28 days. When the age is 60 days and $a_w = 25\%$, the maximum strength can reach 5.36 MPa, which is 3.71 times the strength of ordinary soft soil for 60 days. When the dosage increased from 25% to 30%, the strength growth range of soft soil at 7 and 60 days began to decrease. The linear fitting relationship between a_w and q_u at each age is as follows:

$$\left.\begin{array}{l} q_{u28} = 0.07a_w + q_{u0.7} \, (T = 7d, a_w \leq 30\%) \\ q_{u28} = 0.12a_w + q_{u0.28} \, (T = 28d, a_w \leq 30\%) \\ q_{u60} = 0.15a_w + q_{u0.60} \, (T = 60d, a_w \leq 30\%) \end{array}\right\}. \quad (1)$$

Types $q_{u0.7}$, $q_{u0.28}$, and $q_{u0.6}$ are the strength values of ordinary soft soil at 7 d, 28 d, and 60 d, respectively. The fitting coefficients were 0.96, 0.99, and 0.96, respectively.

In order to facilitate the direct analysis of the enhancement effect of nanosilica powder on soft soil, based on the strength values of ordinary soft soil at 7d, 28 d, and 60d, the growth rate of q_u and a_w of nanosilica powder soft soil at corresponding ages is given, as shown in Table 1 [11].

From the above analysis, it can be observed that the strength of soft soil at various ages can be greatly improved by adding nanosilica powder. When the dosage and age of
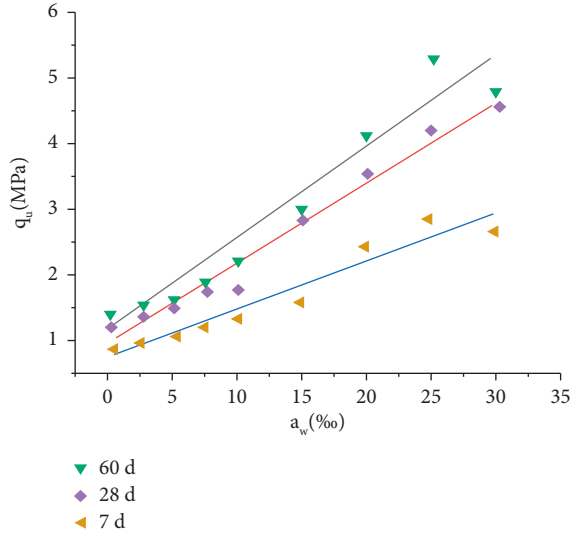
FIGURE 1: Relationship between the parameters of nanosilicon powder and compressive strength.

nanosilica powder are different, the range of strength increase of soft soil is also different.

When the amount of nanosilica powder a_w is less than 5%, the strength of solidified soil at each age increases relatively little. When the dosage is greater than 5%, the strength increases significantly. For the soft soil with nanosilica powder content of 0%–30% and cement content of 15%, the relationship between strength values of the soft soil with nanosilica powder at different ages can be analyzed, as shown in Table 1, and the following fitting relationship can be obtained:

$$\left. \begin{array}{l} q_{u7} = 0.64 q_{u28} \left(a_w \leq 30\% \right) \\ q_{u7} = 0.54 q_{u60} \left(a_w \leq 30\% \right) \end{array} \right\}. \quad (2)$$

Types q_{u7}, q_{u28}, and q_{u60} refer to the strength of the soft soil with nanosilica powder at 7 d, 28 d, and 60 d ages, respectively [12]. It can be seen that the 7 d strength value of the soft soil has reached more than half of the 60 d strength after the doping of silica powder, indicating that the soft soil with silica powder doping has a fast solidification speed and a high early strength.

2.2. Secant Modulus Method.
In this paper, based on the concept of the E-P curve and the Duncan-Chang constitutive model [13], a method is established to calculate the nonlinear secant modulus E_p of soft soil with the E-P curve, and then, the secant modulus E_p is applied to calculate the settlement of foundation caused by lateral deformation. Kondner in 1963, based on the conventional triaxial tests of a large number of soils, obtained the stress-strain relationship of soils by hyperbolic fitting as shown in the following equation:

$$\sigma_1 - \sigma_3 = \frac{\varepsilon_a}{a + b\varepsilon_a}. \quad (3)$$

In the formula, σ_1 is the first principal stress; σ_3 the third principal stress; ε_a is the vertical strain of the sample; a and b are the test constants.

TABLE 1: The strength growth rate of soft soil under different nanosilica powder parameters (unit%).

Age (d)	Nanometer silica powder parameters (%)							
	2.5	5	7.5	10	15	20	25	30
7	14.2	16.6	39.3	45.6	81.2	192.8	252.8	220.7
28	18.5	26.6	41.5	42.9	112.6	203.7	257.3	292.3
60	6.5	8.8	33.9	54.6	112.6	186.2	271.2	228.3

The secant modulus E_p is

$$E_p = \frac{\sigma_1 - \sigma_3}{\varepsilon_a}. \quad (4)$$

Define the failure ratio R_f as

$$R_f = \frac{(\sigma_1 - \sigma_3)_f}{(\sigma_1 - \sigma_3)_{ult}}. \quad (5)$$

Define the stress level s as

$$s = \frac{\sigma_1 - \sigma_3}{(\sigma_1 - \sigma_3)_f} = \frac{(1 - \sin \phi)(\sigma_1 - \sigma_3)}{(2c \cos \phi + 2\sigma_3 \sin \phi)}. \quad (6)$$

Then, (4) can be written

$$E_p = (1 - R_f s) E_{t0}, \quad (7)$$

where E_{t0} is the initial tangent modulus, and its expression is

$$E_{t0} = \frac{1}{(1 - R_f s_0)^2} E_{si}, \quad (8)$$

where S_0 is the initial stress level, that is, the stress level of the soil element under dead weight stress. E_{si} is the compression modulus corresponding to the self-weight stress of the soil element to the sum of the self-weight stress and the total additional stress [14]. Due to $(1 - R_f S_0) < 1$, so $E_{t0} > E_{si}$, to simplify the calculation and to be a little bit safer, set $E_{t0} > E_{si}$; then, the secant modulus E_p is

$$E_p = (1 - R_f S) E_{si}. \quad (9)$$

2.3. Calculation Parameter Determination Method.
In the proposed calculation method, both the settlement calculation under lateral confinement conditions and the settlement calculation caused by lateral deformation need the compression modulus E_{si} under different stress levels, and a complete E-P curve is required to obtain this compression modulus [15]. However, the test reports of some engineering projects do not provide complete E-P, but only provide the initial porosity ratio e_0 and compression modulus E_{s1-2}. Since the above two parameters are commonly used in engineering, they are relatively stable and can better reflect the characteristics of soft soil. Two methods are established to calculate the compression modulus E_{si} under different stress levels from e_0 and E_{s1-2}. Method 1: based on E_{s1-2}, the compression index C_c is deduced, the $e - 1_{gp}$ curve of the normally consolidated soil is obtained from C_c, and then the compression modulus E_{si} under different stress levels is obtained from the $e - 1_{gp}$ curve.

2.3.1. Method 1. For the E-lgp curve of normally consolidated soil [16], p_c is the early consolidation pressure, p_1 is the deadweight stress, e_0 is the initial porosity ratio, and C_{cf} is the in situ compression index. If the in situ compression curve is required, only point B and the in situ compression index C_{cf} can be obtained. The coordinates of point B and the in situ compression index C_{cf} are derived in two parts.

(1) Deduction B. For normally consolidated soil, the early consolidation pressure p_c is

$$P_c = \gamma_{sat}h, \tag{10}$$

where γ_{sat} is the saturated weight of soil mass, and H is the depth of soil collection point. B is γ_{sat} h, e_0.

(2) Derivation of In Situ Compression Index C_{cf}. The compression modulus formula is as follows:

$$E_s = \frac{(1 + e_0)(p_2 - p_1)}{e_1 - e_2}. \tag{11}$$

The compression index formula is as follows:

$$C_c = \frac{e_1 - e_2}{1gp_2 - 1gp_1}. \tag{12}$$

Equations (11) and (12) can be obtained as

$$C_c = \frac{(1 + e_0)(p_2 - p_1)}{((1 + e_0)(p_2 - p_1)/(e_1 - e_2))1g(p_2/p_1)} \tag{13}$$

$$= (1 + e_0)(p_2 - p_1)/(E_s \cdot 1g(p_2/p_1)).$$

If in (13) $p_1 = 100kPa$, $p_2 = 200kPa$, then the compression modulus E_s is E_{s1-2}. (19) is

$$C_{c1-2} = \frac{100(1 + e_0)}{1g2E_{s1-2}}. \tag{14}$$

If the earlier consolidation pressure is $p_c \le 100kPa$, the relationship between C_{c1-2} and C_{cf} can be obtained as follows:

$$C_{c1-2} = C_{cf}. \tag{15}$$

(3) Derivation of Compression Modulus E_{si}. The point B and the in situ compression index C_{cf} deduced above. Thus, the E-lgp curve of soil in situ compression is

$$e = \begin{cases} e_0 \ (P \le \gamma_{sat}h), \\ e_0 - \dfrac{100(1 + e_0)}{1g2E_{s1-2}} \cdot [1gp - 1g(\gamma_{sat}h)] \ (P > \gamma_{sat}h). \end{cases} \tag{16}$$

According to (16), the corresponding pore ratio of soil under dead weight stress is

$$e_1 = e_0. \tag{17}$$

The corresponding pore ratio of soil under the sum of gravity stress and additional stress is

$$e_2 = e_0 - \frac{100(1 + e_0)}{1g2E_{s1-2}} \cdot [1gp - 1g(\gamma_{sat}h)]. \tag{18}$$

Substitute (14) and (15) into the compression modulus formula (17) to obtain the compression modulus of soil at any pressure level:

$$E_{si} = \frac{1g2 \cdot E_{s1-2} \cdot (p - \gamma_{sat}h)}{100[1gp - 1g(\gamma_{sat}h)]}. \tag{19}$$

2.3.2. Method 2. Zhang et al. [17] proposed a method of deducing the E-P curve by AA. The derivation results are as follows:

$$e = e_0 - \frac{(1 + e_0)p}{0.1088E_s + 0.0015E_sp}. \tag{20}$$

Therefore, given the compression modulus E_{s1-2} and the initial porosity ratio e_0, the corresponding porosity ratio under different additional stresses can be obtained. By substituting (20) into (17) for compression modulus calculation, the relation between the compression modulus E_{si} at different stress levels and the additional stress can be obtained, as shown in Figure 2 and Figure 3.

3. The Result

It can be observed from the calculation results that, on both sides of the embankment foundation, the calculated results of various calculation methods are not much different from the measured results [18]. At the center of the embankment foundation, the calculated results are smaller than the measured ones, and the calculated results differ greatly from the measured ones. However, the calculation results of the method considering the settlement caused by lateral deformation (i.e., method (1) and method (2)) are in good agreement with the measured results, and the calculated results are slightly larger and safer than the measured results. For the settlement time curve of the center point of the embankment base, there is also a large error in the standard calculation method from the whole settlement process, while the calculation method considering the settlement caused by lateral deformation (i.e., method (1) and method (2)) is in good agreement with the measured data. The E_{s1-2} and e_0 of soft soil are easy to obtain and the values are stable, and the experience is easy to judge, which can bring great convenience to the calculation [19].

The secant modulus total method is used to reduce the fluctuation of the modulus, and the reliability of the calculation results will be improved. The total method is established to calculate the nonlinear settlement of soft soil foundation based on two parameters commonly used in engineering: initial porosity ratio e_0 and compression modulus E_{s1-2}.
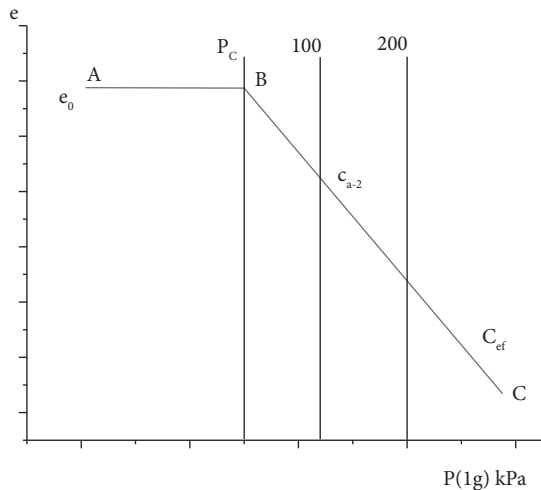
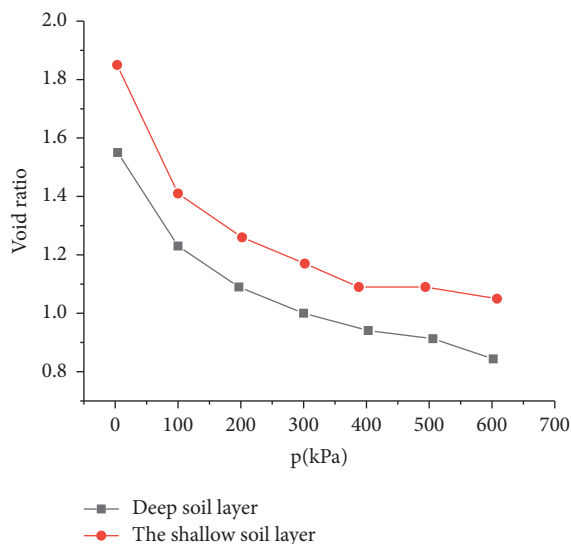FIGURE 2: Relationship between CC1-2 and CCF size.

FIGURE 3: E-P curve of subsoil.

4. Conclusions

Although finite element and other numerical methods are modern advanced methods that can take many factors into account, the accuracy of the calculation cannot be guaranteed because of the error of the constitutive model of nanometer silica silky ooze. E-P curves based on a simple test and combined with the experience coefficient correction are still the main settlement calculation methods of engineering application; in order to improve its precision and experience coefficient uncertainty, carry on test the simplicity of its parameters at the same time, and make up for the inadequacy of current commonly used in the engineering calculation method, this study on the basis of previous work, considering the lateral deformation of the nonlinear settlement calculation method, is put forward. The method can not only improve the calculation accuracy but also give consideration to the engineering ease-of-use, and the effectiveness of the method is preliminarily proved by a case [20].

The strength modification effect is different with different dosages and ages of nanosilicon powder. The 7 d strength of the soft soil with nanosilicon powder can reach more than half of that of 28° and 60 d. Nanosilica powder can improve the early strength of cement soil. When the content is less than 5, the enhancement is not obvious. Nanosilica powder can give full play to its excellent characteristics, refine, and consume $Ca(OH)_2$ crystals produced by cement hydration through the reaction of volcanic ash: this is the main reason for the modification of soft soil with nanosilica powder, and the main modification mechanism of nanosilica powder applied to soft soil. The lateral deformation and resistance to the horizontal force of piles in soft soil foundations are one of the key problems in the lateral stability of embankments. The deformation of soil and piles in the middle and lower parts tends to the outside of embankment, which is not conducive to the stability of embankment. There are many engineering accidents of the instability of soft soil embankments, which is related to the failure of this factor in the design. Due to the deformation (or reinforcement) of the geogrid cushion itself, it can stabilize and fix the pile cap (reduce the deformation of foundation soil), and the deformation of surface soil and pile top tends to the inside of the embankment, which is conducive to the stability of subgrade. Therefore, the nonlinear algorithm is very beneficial to the lateral stability of embankment.

Data Availability

The data used to support the findings of this study are available from the corresponding author upon request.

Conflicts of Interest

The authors declare that they have no conflicts of interest.

References

[1] N. Yan, X. Liu, M. Zhang, X. Bai, and Z. Wang, "Analytical calculation of critical anchoring length of steel bar and gfrp antifloating anchors in rock foundation," *Mathematical Problems in Engineering*, vol. 2021, no. 1, pp. 1–10, 2021.

[2] J. Liu, X. Liu, J. Chen, X. Li, and F. Zhong, "Plasma-catalytic oxidation of toluene on Fe2O3/sepiolite catalyst in DDBD reactor," *Journal of Physics D: Applied Physics*, vol. 54, 2021.

[3] A. E. Sargsyan and E. G. Gukova, "The effectiveness of the implementation of pile foundations i the example of the reactor building of a nuclear power plant with vver-1000," *Structural Mechanics of Engineering Constructions and Buildings*, vol. 16, no. 1, pp. 14–21, 2020.

[4] S. Shriram, B. Nagaraj, J. Jaya, S. Shankar, and P. Ajay, "Deep learning-based real-time AI virtual mouse system using computer vision to avoid COVID-19 spread," *Journal of Healthcare Engineering*, vol. 2021, Article ID 8133076, 8 pages, 2021.

[5] J. Ding, Z. Qin, H. Luo, W. Yang, Y. Wang, and Z. Huang, "Nano-silica modified phenolic resin film: manufacturing and properties," *Nanotechnology Reviews*, vol. 9, no. 1, pp. 209–218, 2020.

[6] O. Afzali-Naniz and M. Mazloom, "Fracture behavior of self-compacting semi-lightweight concrete containing nano-silica," *Advances in Structural Engineering*, vol. 22, no. 10, pp. 2264–2277, 2019.

[7] M. Abd Elrahman, S. Y. Chung, P. Sikora, T. Rucinska, and D. Stephan, "Influence of nanosilica on mechanical properties, sorptivity, and microstructure of lightweight concrete," *Materials*, vol. 12, no. 19, pp. 3078–3088, 2019.

[8] Y. Wang, K. Hu, Y. Zhang, and X. Ding, "Dendritic fibrous nano-silica and titania (dfnst) spheres as novel cata-luminescence sensing materials for the detection of diethyl ether," *RSCAdvances*, vol. 9, no. 68, pp. 39622–39630, 2019.

[9] J. Ma, Y. An, and P. Yu, "Core–shell structure acrylamide copolymer grafted on nano-silica surface as an anti-calcium and anti-temperature fluid loss agent," *Journal of Materials Science*, vol. 54, no. 7, pp. 5927–5941, 2019.

[10] U. Sivasankaran, S. Raman, and S. Nallusamy, "Experimental analysis of mechanical properties on concrete with nano silica additive," *Journal of Nano Research*, vol. 57, pp. 93–104, 2019.

[11] M. E. Mahmoud, M. A. Khalifa, Y. M. El Wakeel et al., "A novel nanocomposite of liquidambar styraciflua fruit biochar-crosslinked-nanosilica for uranyl removal from water," *Bioresource Technology*, vol. 278, pp. 124–129, 2019.

[12] M. Gil-Diaz, E. Rodriguez-Valdes, J. Alonso, D. Baragano, J. R. Gallego, and M. C. Lobo, "Nanoremediation and long-term monitoring of brownfield soil highly polluted with as and hg," *Science of the Total Environment*, vol. 675, pp. 165–175, 2019.

[13] H. Tan, C. Wang, H. Li, D. Peng, C. Zeng, and H. Xu, "Remediation of hexavalent chromium contaminated soil by nano-fes coated humic acid complex in combination with cr-resistant microflora," *Chemosphere*, vol. 242, 2020.

[14] X. Huang, W. Kang, J. Guo et al., "Highly reactive nano-mineral assembly in soil colloids: implications for paddy soil carbon storage," *Science of the Total Environment*, vol. 703, Article ID 134728, 2020.

[15] M. K. A. Kaabar, V. Kalvandi, N. Eghbali, M. E. Samei, Z. Siri, and F. Martínez, "A generalized ML-hyers-ulam stability of quadratic fractional integral equation," *Nonlinear Engineering*, vol. 10, no. 1, pp. 414–427, 2021.

[16] F. J. Manoppo, A. Warouw, J. R. Talumepa, and C. J. Manoppo, "Potential failure of soekarno bridge foundation cause of liquefaction," *Lowland Technology International*, vol. 21, no. 3, pp. 151–158, 2020.

[17] Z. Zhang, Y. Wang, Y. Fang, X. Pan, J. Zhang, and H. Xu, "Global study on slope instability modes based on 62 municipal solid waste landfills," *Waste Management and Research: The Journal for a Sustainable Circular Economy*, vol. 38, no. 12, pp. 1389–1404, 2020.

[18] Z. Huang and S. Li, "Reactivation of learned reward association reduces retroactive interference from new reward learning," *Journal of Experimental Psychology: Learning, Memory, and Cognition*, vol. 48, no. 2, pp. 213–225, 2022.

[19] S. V. Yushchube, I. I. Podshivalov, and A. S. Larionov, "Safety of building constructed on hillside slope," *Vestnik Tomskogo Gosudarstvennogo Arkhitekturno-Stroitel Nogo Universiteta Journal of Construction and Architecture*, vol. 23, no. 1, pp. 126–139, 2021.

[20] R. Huang and X. Yang, "Analysis and research hotspots of ceramic materials in textile application," *Journal of Ceramic Processing Research*, vol. 23, no. 3, pp. 312–319, 2022.